

Flexible conjugated polymer photovoltaic cells with controlled heterojunctions fabricated using nanoimprint lithography

Myung-Su Kim

Department of Materials Science and Engineering, University of Michigan, Ann Arbor, Michigan 48109

Jin-Sung Kim

Electrical Engineering and Computer Science, University of Michigan, Ann Arbor, Michigan 48109

Jae Cheol Cho and Max Shtein

Department of Materials Science and Engineering, University of Michigan, Ann Arbor, Michigan 48109

L. Jay Guo

Electrical Engineering and Computer Science, University of Michigan, Ann Arbor, Michigan 48109

Jinsang Kim^{a)}

Department of Materials Science and Engineering, Chemical Engineering, and Macromolecular Science and Engineering, University of Michigan, Ann Arbor, Michigan 48109

(Received 23 October 2006; accepted 13 February 2007; published online 22 March 2007)

The authors describe conjugated polymer-based photovoltaic devices in which the shape and area of the interface between the electron donor and acceptor layers were controllably varied using nanoimprint lithography. The short circuit current is shown to increase with the interfacial area of the heterojunction, without affecting the open circuit voltage. The fill factor and power conversion efficiency are also shown to increase with donor-acceptor interfacial area. © 2007 American Institute of Physics. [DOI: 10.1063/1.2715036]

Solar cells based on conjugated polymers (CPs) have received considerable attention as an attractive alternative to silicon-based photovoltaic (PV) technology for low-cost solar energy conversion. The potential advantages of polymer-based devices derive from large-area processability of polymers, improved compatibility with low-cost flexible substrates, and the high degree of control over the optoelectronic properties of the CPs. However, the power conversion efficiency remains comparatively low. Among the limiting factors is the trade-off between optical absorption and the diffusion of strongly bound photogenerated electron-hole pairs (excitons) in polymers, prior to their dissociation at the donor-acceptor junction.¹⁻³ This is thought to occur mainly due to the fact that typical exciton diffusion length L_D in conjugated organic compounds is on the order of 10–20 nm,⁴⁻⁹ while the typical optical absorption distance is an order of magnitude greater.

Several techniques have been employed to improve charge separation and transport in organic solar cells, including the use of various electron acceptor compounds, such as crystalline organic dyes, semiconductor nanorods, and C_{60} and its derivatives, in the form of a dispersed second phase in bulk heterojunction (BHJ) CP-based solar cells.¹⁰⁻¹² The BHJ architecture has been demonstrated to improve power conversion efficiency by increasing the area of the interface between the electron donor and acceptor layers through spontaneous phase segregation of the electron donor and acceptor components.¹³⁻¹⁵ Other approaches to control the length scale of phase separation have included patterning using anodic alumina templates,¹⁶ phase separation of block copolymers,¹⁷ and self-organization of nanocrystals in polymer brushes¹⁸ on the nanoscale. However, the spontaneous phase separation that generates the BHJ results in a disor-

dered morphology, with cul-de-sac regions that impede transport of charge to the electrodes.

In an effort to improve charge transport while maintaining a high interfacial area, relatively well-ordered BHJ architectures have been realized using small molecular organic PV systems, fabricated through vapor phase deposition.¹⁰ However, in both the polymer-based disordered BHJ and in the small molecule-based ordered BHJ device architectures, the interface between the donor and acceptor layers remains largely irregular and difficult to characterize precisely. In both cases, the formation of the interface relies on the intermolecular interaction to achieve a morphology close to the desired geometry.

Here we demonstrate a top-down nanofabrication approach to obtaining polymer-based flexible solar cells in which the electron donor and acceptor components are interdigitated with a precisely defined interface geometry. Specifically, we employ a combination of nanoimprinting of the active polymer layers and subsequent solution casting of electron acceptor compounds, with both techniques amenable to high throughput roll-to-roll fabrication.^{9,19,20} The resulting devices exhibit improved power conversion characteristics that are systematically shown to scale with the donor-acceptor interfacial area. The device fabrication approach described here differs from another top-down one, in which nanostructured inorganic electron-transporting materials are infiltrated with energy harvesting and hole-transporting conjugated polymers. In the latter technique, the combination of large molecular weight of the conjugated polymer and the nanoscale dimensions of the channels impede the insertion of polymer chains, resulting in a largely disordered polymer microstructure, and suboptimal hole transport.²¹

In the nanoimprinting approach to fabricating a BHJ organic PV cell, a mold with a nanoscale relief pattern is first prepared by electron beam lithography or optical projection

^{a)}Electronic mail: jinsang@umich.edu

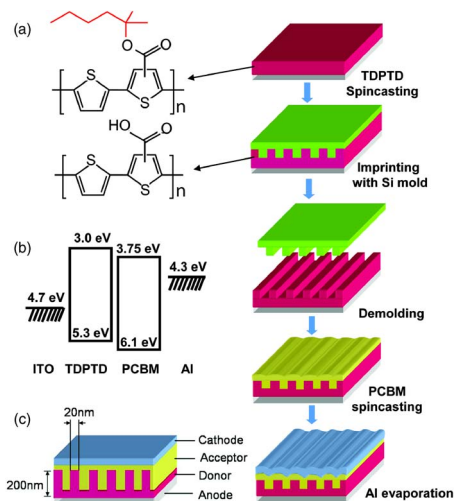


FIG. 1. (Color online) Schematic of a nanoimprinted polymer PV cell, along with the materials and fabrication procedure used to achieve it. Here, on an ITO-coated PET, TDPTD was spin cast and then imprinted with a prepatterned stamp. During this imprinting process the side group of TDPTD was deprotected by heat and TDPTD became insoluble. PCBM was then spin cast and finally Al was evaporated to form the cathode layer. (b) Band structure of the fabricated cell. (c) An idealized diagram of an organic photovoltaic cell structure having an interdigitated donor-acceptor interface.

lithography, and then used to imprint nanoscale features in the polymer of interest. While the lithography techniques used in producing the mold are considered slow and costly, once the mold is fabricated, the multiple replications of nanopatterns in polymer thin films by stamping can be easily achieved. The currently achievable smallest feature size through the nanoimprinting is below 10 nm,^{22,23} on the order of $L_D \approx 10\text{--}20$ nm, suggesting that nanoimprinting can potentially be used to enable a solar cell having the optimized length scale of donor-acceptor layer integration. Here we describe preliminary experiments that examine the use of nanoimprinting to realize ordered BHJ organic PV cells.

Consider the structure of an organic photovoltaic cell illustrated in Fig. 1(c), in which the donor and acceptor domains are interdigitated, allowing efficient absorption of light, improved capture of excitons at the donor-acceptor interface, and a line-of-sight pathway for the extraction of charge carriers.^{15,16} (Heterojunctions consisting of pillar arrays are expected to provide similar advantages, although the grating-shaped interface will suffice for the present discussion.) The fabrication sequence for this device structure is illustrated in Fig. 1. The substrate consists of a flexible in-

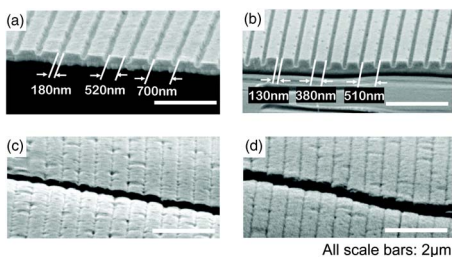


FIG. 2. (Color online) Scanning electron micrographs of (a) TDPTD on a flexible ITO-coated PET, imprinted with a 700 nm period grating. (b) TDPTD on a flexible ITO-coated PET, imprinted with a 510 nm period grating mold. (c) Surface of a PCBM film spin cast onto the imprinted TDPTD (510 nm period). Note that the deep trenches are completely filled with PCBM. (d) Surface of the aluminum (100 nm thick) cathode, evaporated at 2 \AA/s under 10^{-6} Torr onto the PCBM layer. The scale bars shown in the images are $2 \mu\text{m}$.



FIG. 3. (Color online) Photograph of a flexible conjugated polymer solar cell with controlled nanoscale heterojunctions. Inset: TDPTD on a flexible ITO-coated PET, imprinted with a 700 nm period grating mold, diffracting ambient light.

dium tin oxide (ITO)-coated PET foil, onto which a thermally deprotectable polythiophene derivative²⁴ (TDPTD) was spin cast and baked at 120°C for 1 h. The TDPTD surface was then imprinted at 180°C using a preformed stamp, and subsequently coated by the electron acceptor compound from solution. The acceptor consisted of PCBM, spin cast from chlorobenzene, conformally coating the imprinted TDPTD surface. A 100 nm thick aluminum cathode was vacuum deposited onto the PCBM layer to complete the PV cell. The fabricated cells were characterized using an OriolTM solar simulator, at 56 mW/cm^2 illumination intensity.

Two different molds, having 200 nm deep, 510 and 700 nm period gratings, were used to imprint the electron donor layer. As Figs. 2(a) and 2(b) show, the stamp profile was transferred to the polymer with high fidelity in both cases. A photograph of the substrate containing the 700 nm period imprinted electron donor layer is shown in Fig. 3; diffraction of ambient light can be seen in the inset photograph, indicating that the surface relief spans the entire imprinted area.

The photocurrent-voltage response of three different PV cells was compared: (1) control cell with a flat donor-acceptor interface, (2) a nanostructured cell imprinted using the 510 nm pitch grating, and (3) a nanostructured cell imprinted using the 700 nm pitch grating. Figure 4(a) plots the current density J for these devices, clearly showing that as the interface area between the donor and the acceptor increases, the short circuit current density J_{sc} increases. Figure

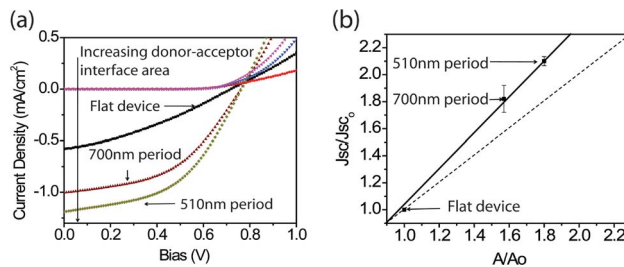


FIG. 4. (Color online) Characterization of the device performance. (a) J - V curves of the flexible conjugated polymer solar cells. The control PV cell (\bullet), the imprinted PV cell having the 700 nm (\blacktriangledown) period, and the imprinted cell having the 510 nm (\blacktriangleleft) period under dark condition. The control cell (\blacksquare), the imprinted cell having the 700 nm (\blacktriangle) period, and the imprinted cell having the 510 nm (\blacklozenge) period under illuminated condition (56 mW/cm^2 intensity). (b) The effect of the vertically oriented interface areas between TDPTD and PCBM is plotted. The interface areas are 0.79 mm^2 for control cell, 1.24 mm^2 for the nanopatterned cell having the 700 nm period, and 1.42 mm^2 for the nanopatterned cell having the 510 nm period. As interface area increases the short circuit current density increases. (J_{sc}/J_{sc_0} , the ratio of the J_{sc} of the cells to the J_{sc} of the control cell; A/A_0 , the ratio of the interface area of the cells to the interface area of the control cell; solid line, linear fit of data; dashed line, 1:1 line of J_{sc}/J_{sc_0} and A/A_0 .)

TABLE I. Performance of the flexible solar cells with controlled nanostructures.

	A/A_o^a	J_{sc} (mA/cm ²)	V_{oc} (V)	FF ^b	PCE (%) ^c
Control cell	1	0.58	0.78	0.34	0.25
Imprinted cell (700 nm)	1.57	1	0.78	0.47	0.66
Imprinted cell (510 nm)	1.80	1.19	0.78	0.48	0.80

^a A/A_o , the ratio of the interface area of the cell to the interface area of the control cell.

^bFF, fill factor is $V_{mp}J_{mp}/V_{oc}J_{sc}$, where V_{mp} and J_{mp} are the voltage and the current density at the maximum power point along the J - V curve.

^cIllumination intensity, 56 mW/cm².

4(b) plots the ratio of J_{sc} for the imprinted devices to that for the planar heterojunction as a function of the ratio of the imprinted interface area to that of the flat interface, A/A_o . While the plot is approximately linear over the three device data points, interestingly, the slope is 1.39. This suggests additional improvements in charge transport that may be realized as a consequence of imprinting the polymer, over the nonimprinted device. Preliminary x-ray diffraction studies (not shown here) on some imprinted conjugated polymer films suggest that additional chain-to-chain ordering may result from the imprinting process. Note that the spin-coated PCBM layer does not completely planarize the imprinted TDPTD layer [Fig. 2(d)], suggesting that mild light scattering may be present and contribute to additional gain in J_{sc} .^{25,26}

The device performance parameters, including the fill factor (FF), open circuit voltage (V_{oc}), and power conversion efficiency (η_{pwr}), are summarized in Table I. The FF is related to the resistance of the cell;²⁷ when the shunt resistance is high and the series resistance is low, a high FF is obtained in the forward current. As Table I shows, the fill factors of the nanostructured cells are 0.47 and 0.48 for the 700 and 510 nm periods, respectively, larger than 0.34 of the control cell that has a flat interface, suggesting improved charge transport in the imprinted device over the nonimprinted one. As a result, the power conversion efficiency of the nanostructured cells with 510 nm (700 nm) period is 3.20 (2.64) times larger than that of the control cell, respectively, even though the actual interface area increases by a factor of 1.75 (1.5).

Note also that the V_{oc} of the device is 0.78 V, greater than the typical V_{oc} of 0.4–0.6 V for a single-junction organic PV cell.^{28,29} One hypothesis is that V_{oc} is controlled by the work functions of the two electrodes.^{30,31} Another hypothesis is that V_{oc} is related to the energy level offsets and doping of the semiconducting materials between the two electrodes.^{32,33} A comparison of the PV device consisting of the layer sequence ITO/TDPTD/PCBM/Al to one consisting of the layer sequence ITO/P3HT/C₆₀/Al supports the latter hypothesis.

In summary, conjugated polymer-based PV cells were fabricated on flexible plastic, with precisely nanostructured donor-acceptor interfaces produced by nanoimprint lithography. The experimentally measured short circuit current increases linearly with the donor-acceptor interfacial area. A significant increase in the fill factor was also observed in the imprinted devices. The rate of increase of J_{sc} , however, exceeds the rate of increase in the interfacial area in corresponding devices, suggesting an additional benefit of the im-

printed structure. This synergistic performance enhancement is believed to originate from the vertically oriented heterojunctions that facilitate charge transport as well as charge separation, ordering of conjugated polymer, and light trapping to the submicron periodic structure of the imprinted solar cells. The detailed, decoupled mechanisms of the synergistic improvement are still under investigation, along with the possibility of achieving finer imprinted features.

One of the authors (J.K.) acknowledges the support of startup funds from the College of Engineering at the University of Michigan, and another author (L.J.G.) thanks support from NSF Grant No. ECS 0424204.

¹C. W. Tang, Appl. Phys. Lett. **48**, 183 (1986).

²N. S. Sariciftci, *Primary Photoexcitations in Conjugated Polymers: Molecular Exciton versus Semiconductor Band Model* (World Scientific, Singapore, 1997).

³B. A. Gregg and M. C. Hanna, J. Appl. Phys. **93**, 3605 (2003).

⁴S. R. Scully and M. D. McGehee, J. Appl. Phys. **100**, 034907 (2006).

⁵D. E. Markov, C. Tanase, P. W. M. Blom, and J. Wildeman, Phys. Rev. B **72**, 045217 (2005).

⁶L. A. A. Pettersson, L. S. Roman, and O. Inganäs, J. Appl. Phys. **86**, 487 (1999).

⁷I. D. Parker, J. Appl. Phys. **75**, 1656 (1994).

⁸G. G. Malliaras, J. R. Salem, P. J. Brock, and J. C. Scott, J. Appl. Phys. **84**, 1583 (1998).

⁹R. N. Marks, J. J. M. Halls, D. D. C. Bradley, R. H. Friend, and A. B. Homes, J. Phys.: Condens. Matter **6**, 1379 (1994).

¹⁰Fan Yang, Max Shtein, and Stephen R. Forrest, Nat. Mater. **4**, 37 (2005).

¹¹W. U. Huynh, J. J. Dittmer, and A. P. Alivisatos, Science **295**, 2425 (2002).

¹²G. Yu, J. Gao, J. C. Hummelen, F. Wudl, and A. J. Heeger, Science **270**, 1789 (1995).

¹³W. C. Goh, K. M. Coakley, and M. D. McGehee, Nano Lett. **5**, 1545 (2005).

¹⁴S. M. Lindner, S. Httner, A. Chiche, M. Thelakkat, and G. Krausch, Angew. Chem., Int. Ed. **45**, 3364 (2006).

¹⁵P. Peumans, S. Uchida, and S. R. Forrest, Nature (London) **425**, 158 (2003).

¹⁶C. Goh, K. M. Coakley, and M. D. McGehee, Nano Lett. **5**, 1545 (2005).

¹⁷S. M. Lindner, S. Httner, A. Chiche, M. Thelakkat, and G. Krausch, Angew. Chem., Int. Ed. **45**, 3364 (2006).

¹⁸H. J. Snaith, Nano Lett. **5**, 1653 (2005).

¹⁹L. J. Guo, J. Phys. D **37**, R123 (2004).

²⁰S. Y. Chou, P. R. Krauss, and P. Renstrom, Appl. Phys. Lett. **67**, 3114 (1995).

²¹K. M. Coakley, Y. Liu, M. D. McGehee, K. L. Frindell, and G. D. Stucky, Adv. Funct. Mater. **13**, 301 (2003).

²²S. Y. Chou, P. R. Krauss, W. Zhang, L. J. Guo, and L. Zhuang, J. Vac. Sci. Technol. B **15**, 2897 (1997).

²³Z. Yu, P. Deshpande, W. Wu, J. Wang, and S. Y. Chou, Appl. Phys. Lett. **77**, 927 (2000).

²⁴J. Liu, E. N. Kadnikova, Y. Liu, M. D. McGehee, and J. M. J. Fréchet, J. Am. Chem. Soc. **126**, 9486 (2004).

²⁵L. S. Roman, O. Inganäs, T. Granlund, T. Nyberg, M. Svensson, M. R. Andersson, and J. C. Hummelen, Adv. Mater. (Weinheim, Ger.) **12**, 3 (2000).

²⁶C. Cocoyer, L. Rocha, L. Sicot, B. Geffroy, R. de Bettignies, C. Sentein, C. Fiorini Debuisschert, and P. Raimond, Appl. Phys. Lett. **88**, 133108 (2006).

²⁷H. Hoppe and N. Serdar Sariciftci, J. Mater. Res. **19**, 1924 (2004).

²⁸G. Li, V. Shrotriya, J. Huang, Y. Yao, T. Moriarty, K. Emery, and Y. Yang, Nat. Mater. **4**, 864 (2005).

²⁹W. Ma, C. Yang, X. Gong, K. Lee, and A. J. Heeger, Adv. Funct. Mater. **15**, 1617 (2005).

³⁰V. D. Mihailetschi, P. W. M. Blom, J. C. Hummelen, and M. T. Rispen, J. Appl. Phys. **94**, 6849 (2003).

³¹H. Frohne, S. E. Shaheen, C. J. Brabec, D. C. Müller, N. S. Sariciftci, and K. Meerholz, ChemPhysChem **9**, 795 (2002).

³²C. M. Ramsdale, J. A. Barker, A. C. Arias, J. D. MacKenzie, R. H. Friend, and N. C. Greenham, J. Appl. Phys. **92**, 4266 (2002).

³³J. A. Barker, C. M. Ramsdale, and N. C. Greenham, Phys. Rev. B **67**, 075205 (2003).